JOURNAL OF CHEMICAL INFORMATION AND MODELING

Article

pubs.acs.org/jcim

Improving the Scoring of Protein−Ligand Binding Affinity by Including the Effects of Structural Water and Electronic Polarization

Jinfeng Liu,[†] Xiao He,*[,†] and John Z. H. Zhang*[,†,‡]

[†]State Key Laboratory of Precision Spectroscopy and Department of Physics, Institute of Theoretical and Computational Science, East China Normal University, Shanghai 200062, China

[‡]Department of Chemistry, New York University, New York, New York 10003, United States

Supporting Information

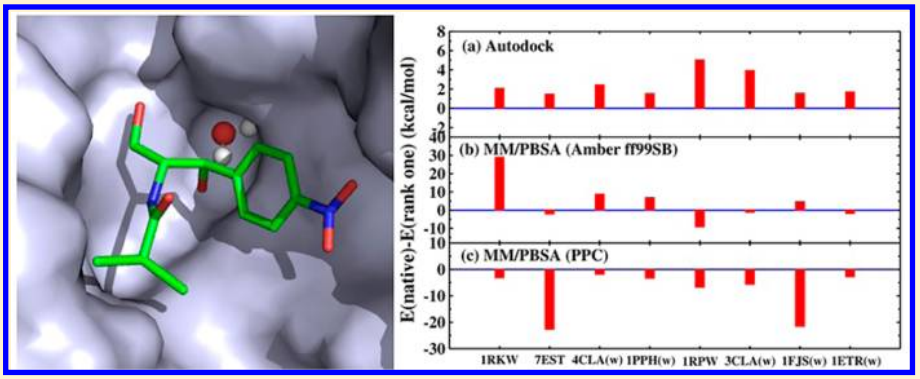

ABSTRACT: Docking programs that use scoring functions to estimate binding affinities of small molecules to biological targets are widely applied in drug design and drug screening with partial success. But accurate and efficient scoring functions for protein−ligand binding affinity still present a grand challenge to computational chemists. In this study, the polarized protein-specific charge model (PPC) is incorporated into the molecular mechanics/Poisson−Boltzmann surface area (MM/PBSA) method to rescore the binding poses of some protein−ligand complexes, for which docking programs, such as Autodock, could not predict their binding modes correctly. Different sampling techniques (single minimized conformation and multiple molecular dynamics (MD) snapshots) are used to test the performance of MM/PBSA combined with the PPC model. Our results show the availability and effectiveness of this approach in correctly ranking the binding poses. More importantly, the bridging water molecules are found to play an important role in correctly determining the protein−ligand binding modes. Explicitly including these bridging water molecules in MM/PBSA calculations improves the prediction accuracy significantly. Our study sheds light on the importance of both bridging water molecules and the electronic polarization in the development of more reliable scoring functions for predicting molecular docking and protein−ligand binding affinity.

1. INTRODUCTION

Molecular docking plays an important role in drug design and discovery with the universal application of docking programs, such as Glide,[1] Autodock,[2] FlexX,[3] and GOLD.[4] When these programs are utilized prior to experimental screening, they are usually considered as powerful computational filters to reduce labor and cost. All of these docking programs explore various docked conformations and determine the tightness of interactions between the protein and the ligand, but the performance on predicting the experimentally observed binding poses is not always satisfying. As is widely accepted, the real bottleneck on obtaining the reliable docking result lies in the scoring functions.[5−10] As a matter of fact, considerable efforts have been devoted to the development of approximate computational methods for describing protein−ligand interactions more accurately, but it still lacks a universal scoring function which works reliably for all or most of protein−ligand systems.[11,12] For some particular protein−ligand systems, most of the widely used docking programs are incapable of predicting the correct binding modes, imposing great challenge on the effectiveness of computer-aided drug design. Therefore, improved methods for predicting protein−ligand binding affinities are desperately needed.

Among the approximate methods, the molecular mechanics/Poisson−Boltzmann surface area (MM/PBSA) approach is attractive because it does not contain any parameters that vary for different protein−ligand systems and it involves a set of physically well-defined energy terms.[13−19] The validity of such an approach has been explored in previous studies.[13,20,21] In particular, Kuhn et al. validated the MM/PBSA approach on different biological systems by putting forward the idea of using single-minimized structure instead of MD trajectories.[22] Moreover, Hou et al. systematically evaluated the performance

Received: January 29, 2013
Published: May 7, 2013

of MM/PBSA on predicting the absolute binding affinity for protein−ligand complexes and the accuracy of identifying the correct binding poses generated from molecular docking programs.[23,24]

The accuracy of MM/PBSA approach for predicting protein−ligand binding affinity relies on the accuracy of force field, in addition to other factors. It is known that current nonpolarizable force fields, for example, CHARMM and AMBER, often fail to give accurate representation of the electrostatics of the specific protein environment, which is highly inhomogeneous and protein-specific. Recently, polarized protein-specific charges (PPC) based on a fragmentation scheme[25−27] for electronic structure calculation of biomolecules and the continuum dielectric model for the solvent in a self-consistent fashion was developed.[28] Since PPC correctly describes the polarized electrostatic state of a protein at a given structure, it is able to give a more accurate description of the mutual electrostatic polarization effect for protein−ligand binding, resulting in better description of electrostatic interactions between protein and ligand. It has been demonstrated in a number of applications that PPC gives significantly better agreement with experimental data than standard nonpolarizable force fields in protein−ligand binding affinity calculations using MM/PBSA.[29] Previous studies by Tong et al. highlight that the electronic polarization of protein plays a critical role in stabilizing the β-sheet (Thr113−Arg122) at the binding site and makes a substantial contribution to the binding free energy of avidin−biotin.[30] In this work, we apply the PPC charge model for MD simulations and MM/PBSA calculations on ranking the protein−ligand binding poses generated from molecular docking.

The effect of bridging water molecules between the protein and ligand attracts more and more attention recently. These water molecules are considered to play an important role in mediating the interaction between protein and ligand.[5,31−38] While only a few scoring functions explicitly take the water-mediated protein−ligand interactions into consideration,[39−42] explicitly including the bridging water molecules in molecular docking and scoring function may be crucial for correctly predicting the binding poses. Hence, in this study, we treat the bridging water molecules as part of the receptor in the docking process and MM/PBSA calculation of binding affinities.

In this work, we applied the MM/PBSA method using both Amber ff99SB and PPC charge models to rescore the docking conformations of some protein−ligand systems, for which Autodock is not able to predict their experimentally observed (native) binding poses. In those cases, the best-scored conformation (rank one) whose predicted binding affinity is most favorable, has a root-mean-squared deviation (RMSD) value larger than 2.0 Å with respect to the experimentally observed bound structure.[5] Our aim is to find a rigorous method to correctly rank the native structure, which in principle, should have higher binding affinity than the rank one binding pose predicted by Autodock. The MM/PBSA calculations are carried out for both the rank one and native structures. We also explicitly treat the bridging water molecules as part of the receptor in the molecular docking and MM/PBSA calculations, and compare with the results by neglecting the structural water molecules. Finally, new physical insights into accurate prediction of protein−ligand binding affinity will be discussed.

2. COMPUTATIONAL APPROACH

A. Preparation of the Protein−Ligand Complexes. The test set used in this study consists of eight protein−ligand complexes (PDB id 1FJS, 1ETR, 1RPW, 1RKW, 3CLA, 4CLA, 1PPH, 7EST, respectively). For each of the protein−ligand systems, the ligand molecule binds to the target protein noncovalently, and no metal ions were found in the binding pocket. Coordinates of all the complexes were downloaded from the Protein Data Bank (PDB). The structures of protein and ligand were then extracted from each complex separately. Hydrogen atoms were added to the protein using the Leap module in AMBER11.[43] The amine groups were fully protonated (Lys and Arg residues and N-terminal), and the carboxylic groups were deprotonated (Asp and Glu residues and C-terminal). All His residues were left neutral and protonated at the ND1 or NE2 position base on the local electrostatic environment. Partial charges of the protein are assigned with the Amber ff99SB force field.[44] For each ligand, hydrogen atoms were added using Discovery Studio. The geometry of ligand was optimized at the HF/6-31G* level. Subsequently, force field parameters of ligand were obtained using ANTECHAMBER module[45] based on the generalized Amber force field (GAFF)[46] with the HF/6-31G* RESP charges.[47,48] (See Table S1 of the Supporting Information.) All the ab initio calculations were carried out using Gaussian09 program.[49] For five complexes (namely, 1FJS, 1ETR, 3CLA, 4CLA, 1PPH), there are bridging water molecules mediating the protein−ligand interaction in the binding pocket. We also keep them as part of the receptor in the molecular docking and MM/PBSA calculations, and compare with the corresponding results obtained without structural waters.

B. Docking and Geometry Optimization of Protein−Ligand Complexes. Autodock program[2] (version 4.2) was employed to generate an ensemble of docked conformations for each ligand bound to its target. We use the genetic algorithm (GA) for conformational search. To explore the conformational space of the ligand as completely as possible, we perform 100 individual GA runs to generate 100 docked conformations for each ligand. The size of the docking box is 60 Å × 60 Å × 60 Å, which is centered at the mass center of the experimentally observed position of the ligand. The box with grid spacing of 0.375 Å, is large enough to enclose the largest binding pocket observed in the entire test set. The protein structure is kept fixed during molecular docking.

For each complex, the rank one docking pose and the native binding pose were optimized in the binding pocket, while the receptor was kept fixed. Geometry optimization was performed with 1500 steps of the steepest descent algorithm followed by 1500 steps of a conjugated gradient method using the Sander module of AMBER11.[43] The cutoff for the nonbonded interaction was set to 200 Å.

C. Derivation of PPC Charges. The PPC charges are fitted to electrostatic potentials by fragment quantum-mechanical calculations using an iterative approach as described in ref 28. Specifically, for each protein structure, a series of minimizations using the Amber ff99SB force filed was carried out to remove close contacts. The minimized structure was then used to calculate PPC charges by the MFCC-PB computational protocol: the Poisson−Boltzmann (PB) solver Delphi[50] is first used to calculate the induced charges on the solute−solvent interface which is defined using a probe radius of 1.4 Å.[51] The polarization of each protein fragment due to the rest

of the protein fragments and the solvent are explicitly included as external point charges in the fragment quantum calculation. The electrostatic potentials are saved and a standard two-stage RESP fitting procedure is used to fit effective point charges of protein.[52,53] The newly fitted atomic charges are passed to the next round of the fragment quantum calculation. The calculated corrected reaction field energy from Delphi using the fitted charges is taken as the convergence criterion and this process is iterated until its variation is smaller than a certain threshold. Usually the criterion will be reached within five iterations. The solvent dielectric constant is set to 80, and a grid density of 4.0 grids/Å is used in numerically solving the PB equation. The quantum-chemical calculations on the protein fragments are performed using density functional theory at the B3LYP/6-31G* level.

D. MD Simulations. Two separate MD simulations were performed for each system using the standard Amber ff99SB and PPC charge models, respectively. In the simulation using PPC, the atomic charges of the Amber ff99SB force field are simply replaced by PPC, while the rest of the ff99SB parameters are retained. In MD simulations, each complex is immersed in a periodic rectangular box of TIP3P water molecules. The distance from the surface of the box to the closest atom of the solute is set to 10 Å. Counterions are added to neutralize the system. The detailed number of TIP3P waters added along with the number and type of counterions added to each complex are shown in Table S2 of the Supporting Information. The particle mesh Ewald (PME) is employed to treat the long-range electrostatic interactions.[54] Two steps of minimizations are carried out to optimize the initial structure. In the first step, only the solvent molecules and hydrogen atoms of the protein−ligand complex are optimized using the steepest descent algorithm followed by the conjugate gradient method. In the second step, the entire system is energy-minimized until convergence is reached. After the two-step minimization, the system is then gradually heated from 0 to 300 K in 100 ps (NVT ensemble), followed by 1 ns NPT simulation at 300 K and 1 atm with a time step of 2 fs.[30] The SHAKE algorithm is employed to restrain all bonds involving hydrogen atoms.[55] A 10 Å cutoff for the van der Waals interactions was adopted. Langevin dynamics[56] was applied to regulate the temperature with a collision frequency of 2.0 ps^{-1}. The pressure was controlled by the isotropic position scaling protocol. All the MD simulations were performed with AMBER11 program.[43]

E. MM/PBSA Calculation of the Protein−Ligand Binding Affinity. The binding free energy of protein−ligand complex is calculated using MM/PBSA method[16,57]

$$\Delta G_{\text{bind}} = G_{\text{complex}} - G_{\text{receptor}} - G_{\text{ligand}} \quad (1)$$

$$= \Delta E_{\text{MM}} + \Delta G_{\text{PB}} + \Delta G_{\text{nonpolar}} - T\Delta S \quad (2)$$

where ΔE_{MM} is the gas-phase interaction energy between protein and ligand, including the electrostatics and van der Waals energies; ΔG_{PB} and $\Delta G_{\text{nonpolar}}$ are the polar and nonpolar components of the desolvation energy, respectively; and $T\Delta S$ is the change of conformational entropy upon ligand binding. In this study, the change of conformational entropy is not included in the MM/PBSA calculations because of the large fluctuation of this term. A large number of snapshots are usually required for reliable evaluation of the conformational entropy. In addition, since we focus on the relative binding affinity between the native and rank one structure other than the absolute value, the contribution of conformational entropy upon binding is approximately treated to be equal, when a ligand is bound to the same target with different binding conformations. In MM/PBSA calculation, the value of the exterior dielectric constant is set to 80, and the solute dielectric constant is set to 1. The nonpolar solvation term is calculated from the solvent-accessible surface area (SASA):[58] $\Delta G_{\text{nonpolar}} = \gamma \times \Delta\text{SASA}$. [where γ = 0.0072 kcal/(mol·Å^2), and the unit of ΔSASA is Å^2.] When the bridging water molecules are explicitly included in the binding affinity calculation, they are treated as part of the receptor. To obtain the ensemble-averaged binding free energies, 50 snapshots were evenly extracted along the MD simulation after the systems were well equilibrated.

For MM/PBSA calculations using PPC, the electrostatic interaction energy in ΔE_{MM} of eq 2 is calculated using the following equation as derived in ref 59

$$\Delta E_{\text{ele}} = \frac{1}{2} \sum_{i \in P, j \in L} \left[\frac{q_{i0} q_{j0}}{R_{ij}} + \frac{q_i q_j}{R_{ij}} \right] \quad (3)$$

where ΔE_{ele} is in kcal/mol. i, j represent the atom in protein (P) and ligand (L), respectively. R_{ij} is the distance between atoms i and j. q_{i0} and q_{j0} are the PPC charges of atom i and j in the unbound state (protein and ligand are infinitely separated), while q_i and q_j are their PPC charges in the bound state of protein−ligand complex. ΔG_{PB} of eq 2 is calculated as

$$\Delta G_{\text{PB}} = \Delta G_{\text{PL,PB}} - \Delta G_{\text{P,PB}} - \Delta G_{\text{L,PB}} \quad (4)$$

where $\Delta G_{\text{PL,PB}}$ denotes the solvation energy of protein−ligand complex calculated using PPC charges of the bound state with the PB model and $\Delta G_{\text{P,PB}}$ and $\Delta G_{\text{L,PB}}$ represent the solvation energy of protein and ligand calculated using PPC charges of the unbound state, respectively. Since the van der Waals interaction energy and $\Delta G_{\text{nonpolar}}$ of eq 2 do not depend on the point charges, these two terms for PPC calculations are the same as those for Amber ff99SB calculations.

3. RESULTS AND DISCUSSION

A. Molecular Docking without Structural Water. In the first round of molecular docking, all the structural water molecules were removed. As shown in Table 1, the Autodock program was unable to pick out the native binding conformation as the most favorable pose for the eight systems we have chosen in this study. All the rank one binding poses have RMSDs greater than 2.0 Å with respect to the native

Table 1. Rank for the First Binding Pose Whose RMSD is Less than 2.0 Å Using Autodock Program with Respect to the Native Structure[a]

system	without bridging waters	with bridging waters
3CLA	>100	96 (1.77)
4CLA	100 (1.08)	82 (1.06)
1PPH	12 (1.20)	22 (1.99)
1FJS	59 (1.29)	1 (1.67)
1ETR	21 (0.93)	1 (0.60)
1RKW	3 (1.40)	*b*
1RPW	>100	*b*
7EST	8 (0.81)	*b*

[a]The molecular docking was performed with and without bridging water molecules, respectively. The RMSD (Å) of the pose is given in parentheses. [b]No bridging water molecules exist in the crystal structure.

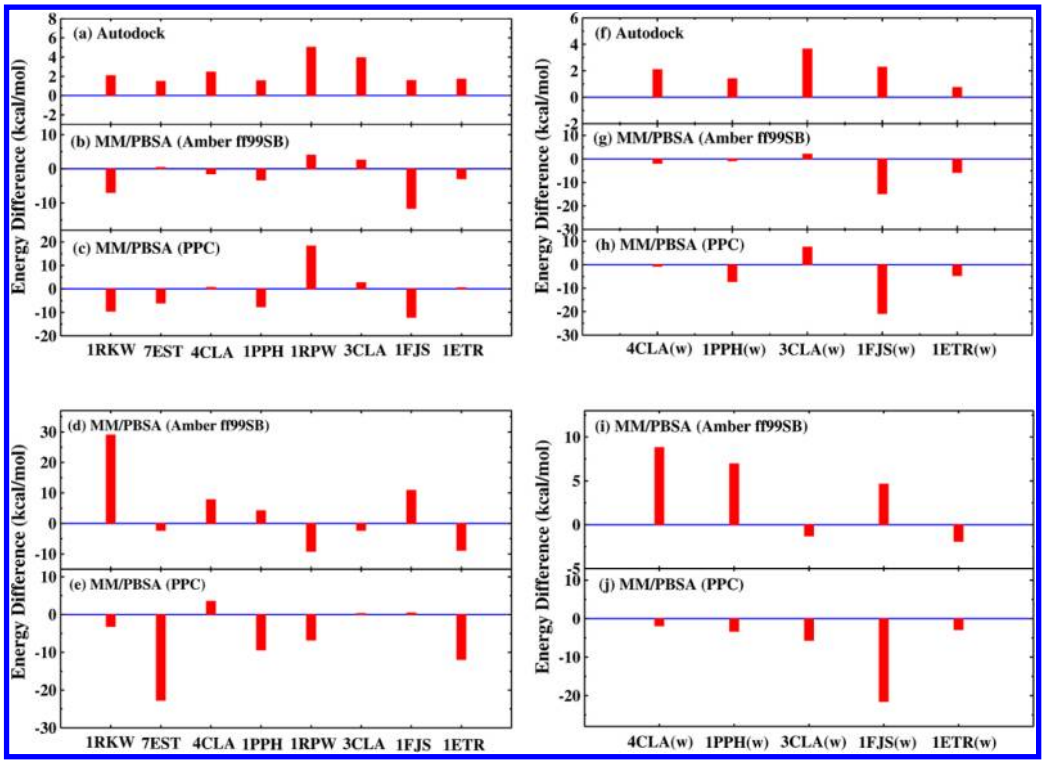

Figure 1. Free energy difference between the native binding structure and the rank one pose predicted by Autodock ($\Delta G_{\text{Native}} - \Delta G_{\text{Rank one}}$). The results obtained from Autodock are shown in panels a and f; panels b–e and g–j present the results calculated using MM/PBSA. Panels b, c, g, and h are based on the single minimized conformation. Panels d, e, i, and j are an ensemble averaging over 50 snapshots selected from MD simulation. The MM/PBSA calculations with Amber ff99SB charges are shown in panels b, d, g, and i, while the MM/PBSA calculations with PPC charges are shown in panels c, e, h, and j, respectively. The notation "(w)" represents that the bridging water molecules are explicitly included in calculations and treated as part of the receptor.

Table 2. Calculated MM/PBSA Free Energies (in kcal/mol) with Amber ff99SB and PPC Charges Based on Single Minimized Structure and Comparison with Autodock Scores[a]

	MM/PBSA				Autodock	
	Amber ff99SB		PPC			
system	native	rank one	native	rank one	native	rank one
1RKW	**−49.30**	**−42.36**	**−49.08**	**−39.60**	−5.36	−7.44 (2.27)
7EST	−34.62	−35.01	**−36.49**	**−30.50**	−5.21	−6.70 (4.65)
4CLA	**−19.04**	**−17.58**	−11.82	−12.53	−1.53	−3.99 (6.25)
1PPH	**−54.86**	**−51.60**	**−60.83**	**−53.21**	−8.03	−9.58 (2.80)
1RPW	−49.81	−53.82	−45.51	−63.85	−2.63	−7.67 (3.21)
3CLA	−12.28	−14.86	−7.24	−9.96	−0.61	−4.56 (6.47)
1FJS	**−67.17**	**−55.54**	**−74.19**	**−62.05**	−7.89	−9.46 (2.23)
1ETR	**−48.66**	**−45.73**	−48.70	−49.25	−8.62	−10.33 (4.41)

[a]The RMSD (Å) of the rank one structure (with the highest score given by Autodock) with respect to the corresponding native structure is given in parentheses. The bridging water molecules were excluded in MM/PBSA calculations. The numbers are in bold face if the free energy of native structure is lower than that of the rank one structure.

structures. Wang et al. have made an extensive test of eleven scoring functions for molecular docking, and none of them was able to predict the top-rank conformation for 3CLA and 4CLA within an RMSD threshold of 2.0 Å.[5] Moreover, Hou et al. also reported that Autodock and MM/PBSA failed to identify the correct binding mode for these two systems.[24] In their studies, structural water molecules mediating the protein–ligand interactions were all removed in docking and MM/PBSA calculations.

B. Rescoring of Binding Free Energies Using MM/PBSA without Structural Waters. For the eight systems, we applied the MM/PBSA method to rescore the rank one and native structure for each protein–ligand complex. We first calculate the binding free energies based on the single minimized structure. Figure 1a–1c shows the free energy differences between the native and rank one structures. As one can see from the figure, MM/PBSA successfully identifies the native conformations for 5 (1RKW, 4CLA, 1PPH, 1FJS, 1ETR) of the 8 complexes using Amber ff99SB charges. The performance of PPC is slightly worse than Amber ff99SB. PPC predicts that the rank one structures are more favorable than the native structures for 1ETR and 4CLA, while the Amber ff99SB identifies the correct binding poses. But for 7EST, PPC successfully picks out the correct binding pose,

dx.doi.org/10.1021/ci400067c | J. Chem. Inf. Model. 2013, 53, 1306–1314

while Amber ff99SB fails. For two systems (1RPW and 3CLA), both Amber ff99SB and PPC give lower binding free energy for the rank one structure than the native structure. The calculated binding energies by Autodock and MM/PBSA based on the single minimized structure are shown in Table 2. The detailed contributions to the total binding free energies from electrostatics, van der Waals interaction, polar and nonpolar desolvation energy are shown in Table S3 of the Supporting Information. Although MM/PBSA calculation based on the minimized structure does not correctly predict the binding modes for all eight systems, it shows a significant improvement over Autodock scores.

MM/PBSA calculations over 50 snapshots from MD simulation were also carried out to calculate binding free energies for these eight systems. As shown in Figure 1d, the ensemble-averaged free energies based on the Amber ff99SB for 7EST, 1RPW, and 3CLA are able to recognize the native structure as opposed to the results based on the single optimized conformation. For 7EST, the ensemble-averaged binding free energies using Amber ff99SB charges are −27.07 and −24.82 kcal/mol for the native and rank one conformations, respectively (see Table 3). As for 1RPW and

Table 3. Calculated MM/PBSA Free Energies (in kcal/mol) with Amber ff99SB and PPC Charges Based on 50 Snapshots Selected from MD Simulation[a]

	Amber ff99SB		PPC	
system	native	rank one	native	rank one
1RKW	−20.43	−49.44	**−32.30**	**−29.14**
7EST	**−27.07**	**−24.82**	**−43.36**	**−20.63**
4CLA	−9.51	−17.32	−7.79	−11.34
1PPH	−49.21	−53.41	**−54.13**	**−44.76**
1RPW	**−44.75**	**−35.60**	**−43.27**	**−36.51**
3CLA	**−12.91**	**−10.65**	−13.55	−13.81
1FJS	−43.14	−54.03	−60.17	−60.62
1ETR	**−45.47**	**−36.63**	**−53.58**	**−41.68**

[a]The bridging water molecules were excluded in MM/PBSA calculations.

3CLA, they are −44.75 (native) versus −35.60 (rank one) kcal/mol and −12.91 (native) versus −10.65 (rank one) kcal/mol, respectively. However, MM/PBSA with Amber ff99SB charges gives lower binding free energies for the rank one structures than the native structures for other four systems (1RKW, 4CLA, 1PPH, 1FJS). On the contrary, MM/PBSA with PPC charges improves the successful rate of identifying the correct binding poses, with three complexes (4CLA, 3CLA, 1FJS, see Figure 1e) that MM/PBSA with PPC fails to recognize the native binding mode. Thus, we conclude that MD simulation does not always improve the performance of MM/PBSA predictions on the binding free energy based on the nonpolarizable Amber ff99SB charge model. In contrast, for the PPC charge model, the ensemble-averaged binding free energy over multiple snapshots generally gives more reliable result than that calculated on the single optimized structure.

C. Molecular Docking with Structural Water Molecules in the Binding Pocket. There are five protein−ligand complexes (1ETR, 1FJS, 1PPH, 4CLA, 3CLA) containing bridging water molecules. Neglecting the bridging water molecules may lead to the failure of predicting the binding mode. Hence, we redock these systems by keeping the structural water molecules in the binding site as part of the receptor. As shown in Table 1, Autodock identified the correct binding conformations for two systems: 1ETR and 1FJS (see Figure 2). For 1ETR, the RMSD of the best-scored

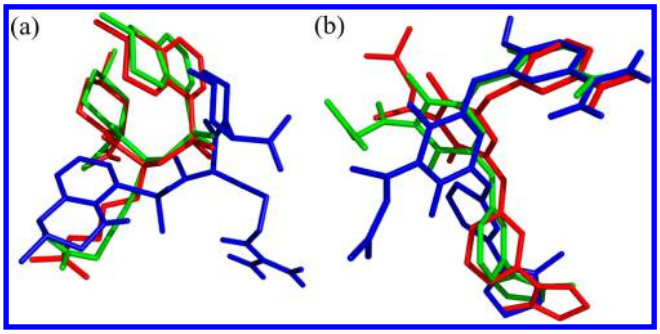

Figure 2. Superposition of best-scored conformations generated by Autodock with and without the bridging water molecules for (a) 1ETR and (b) 1FJS, respectively. The conformations generated with and without bridging water molecules are shown in red and blue sticks, respectively. The experimentally observed conformation is colored in green.

conformation generated with bridging water molecules is 0.60 Å, which is much smaller than that (4.41 Å, see Table 2) of the best-scored conformation generated without structural waters. The result is similar for 1FJS, with the RMSD of 1.67 Å with structural waters versus 2.23 Å without structural waters. Figure 3 shows the ligand binding poses for the native and rank one

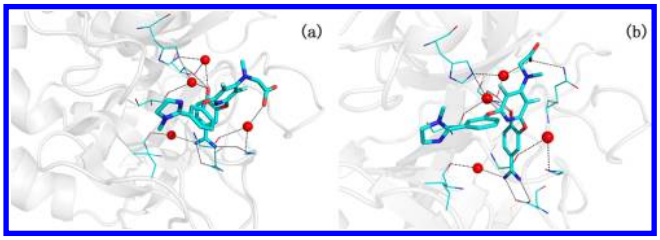

Figure 3. Protein−ligand binding modes for (a) the native structure and (b) the best-scored pose predicted by Autodock for 1FJS, respectively. The hydrogen bonds are shown in dashed lines. The ligand and residues are shown in sticks and lines, respectively. The red spheres represent the bridging water molecules.

structures of 1FJS. The native structure has four structural water molecules bridging between the ligand and protein. In contrast, there are only three structural waters acting as bridging water molecules in the binding site for the rank one binding pose. However, Autodock is still unable to correctly predict the binding poses for the other three systems (1PPH, 3CLA, and 4CLA) by including the bridging water molecules (see Table 1). Furthermore, as shown in Table 4 and Figure 1f, although some of the binding poses are correctly identified, all the binding free energies of rank one poses are predicted to be lower than the native structures by Autodock score. It clearly shows that the deficiency of the scoring function is the main cause for the failure of identifying the correct binding poses.

The estimated binding free energies by Autodock are also affected significantly after considering the bridging water molecules. These structural water molecules enhance the tightness of interactions between protein and ligand, especially in the native structure. As can be seen from Tables 2 and 4, the Autodock scores for the native and rank one structure of 1ETR is −9.98 and −10.72 kcal/mol with considering the bridging

Table 4. Comparison of the Calculated MM/PBSA Free Energies (in kcal/mol) Based on Single Minimized Structure[a]

	MM/PBSA					
	Amber ff99SB		PPC		Autodock	
system	native	rank one	native	rank one	native	rank one
4CLA(w)	**−18.55**	**−16.66**	**−15.73**	**−15.06**	−1.94	−4.03 (8.45)
1PPH(w)	**−57.73**	**−56.95**	**−68.70**	**−61.54**	−8.22	−9.62 (2.73)
3CLA(w)	−14.36	−16.38	−2.51	−10.04	−0.70	−4.34 (2.90)
1FJS(w)	**−78.17**	**−63.35**	**−90.62**	**−69.84**	−8.38	−10.65 (1.67)
1ETR(w)	**−61.40**	**−55.63**	**−62.88**	**−58.19**	−9.98	−10.72 (0.60)

[a]The notation "(w)" represents that the bridging water molecules are explicitly included in calculations. The bridging water molecules are treated as part of the receptor. The RMSD (Å) of the rank one structure (with the highest score given by Autodock) with respect to the corresponding native structure is given in parentheses.

water molecules, compared to the corresponding values of −8.62 and −10.33 kcal/mol without bridging water molecules, respectively. These bridging water molecules increase the binding free energy for the native structure by 1.36 kcal/mol, which is more than 0.39 kcal/mol for the rank one structure. The same tendency is also found for 4CLA, 1PPH, and 3CLA. Nevertheless, for 1FJS, the bridging water molecules contribute more to the binding free energy for the rank one structure than that for the native structure. To summarize, structural waters play an important role in the protein−ligand binding. Explicitly including the effect of bridging water molecules is critical to improving the accuracy of scoring functions.

D. Rescoring of Binding Free Energies Using MM/PBSA with Structural Water Molecules. As discussed in previous sections, when we utilize the ensemble-averaged MM/PBSA binding free energy as the scoring function, the failure of identifying the correct binding poses happens to the protein−ligand complexes, which mostly have bridging water molecules in the binding site. For 1ETR, 1FJS, 1PPH, 4CLA, and 3CLA, which contain bridging water molecules in the crystal structures, we recompute their binding free energies using MM/PBSA by assigning the structural waters as part of the receptor. The MM/PBSA results calculated using Amber ff99SB and PPC for the single minimized conformation and ensemble averaging are shown in Table 4 and 5, respectively.

Table 5. Comparison of MM/PBSA Free Energies (in kcal/mol) Based on 50 Snapshots Selected from MD Simulation[a]

	Amber ff99SB		PPC	
system	native	rank one	native	rank one
4CLA(w)	−8.07	−16.88	**−9.77**	**−7.89**
1PPH(w)	−50.33	−57.27	**−53.52**	**−50.19**
3CLA(w)	**−5.75**	**−4.48**	**−15.50**	**−9.83**
1FJS(w)	−53.94	−58.57	**−75.76**	**−54.23**
1ETR(w)	**−51.02**	**−49.12**	**−50.85**	**−48.00**

[a]The notation "(w)" represents that the bridging water molecules are explicitly included in calculations. The bridging water molecules are treated as part of the receptor.

For MM/PBSA calculations on the single minimized conformation, it was still unable to predict the correct binding mode of 3CLA for both Amber ff99SB and PPC charge models (compare Figure 1g and 1h with Figure 1b and 1c); however, the MM/PBSA binding free energy of the native structure becomes lower than the rank one structure for 4CLA and 1ETR, based on the PPC model after the bridging water molecules are explicitly included. It is worth noting that, unlike MM/PBSA, the linear interaction energy (LIE)[60,61] and linear response approximation (LRA) methods[62,63] do not require the explicit treatment on the bridging water molecules. Nevertheless, the LIE and LRA approaches usually need a large training set to fit the coefficient for each individual energy term empirically.

Figure 1i and 1j shows the relative binding free energies based on ensemble averaging over 50 snapshots selected from MD simulation with Amber ff99SB and PPC, respectively. As can be seen from the figure, by including the bridging waters, MM/PBSA with Amber ff99SB recognizes the correct binding modes for 3CLA and 1ETR, but it is still incapable of identifying the correct binding poses for three systems (4CLA, 1PPH, and 1FJS). However, MM/PBSA with the PPC model correctly recognizes the native binding poses for all the studied systems after including the structural waters, whereas it was unable to identify the correct binding poses for three systems (4CLA, 3CLA, and 1FJS) using the same approach without the structural waters (compare Figure 1j and 1e). Since the polarized protein-specific charges correctly represent the electronically polarized state of the protein and provide accurate electrostatic interaction near the native structure, the electronic polarization effect not only influences the direct calculation of the MM/PBSA binding free energy for protein−ligand complexes but also offers a better conformational sampling for proteins, which is an essential prerequisite for obtaining any ensemble-averaged property of proteins. Including the effects of both bridging water molecules and the electronic polarization of protein gives perfect prediction for MM/PBSA calculations.

As shown in Tables 3 and 5, for 1FJS, which has 4 bridging water molecules, the total binding free energy of the native structure is −75.76 kcal/mol when bridging water molecules are explicitly included in the MM/PBSA calculation with PPC, as compared to −60.17 kcal/mol without considering the structural waters. As one can see from Figure 3, each bridging water molecule forms a stable hydrogen bond with the ligand and mediates the interactions between the protein and ligand. These structural waters have a contribution of −15.59 kcal/mol to the total binding free energy, which makes the protein−ligand binding more attractive. For 1FJS without structural waters, the electrostatics, van der Waals interaction and polar desolvation energy contributions to the binding of the native structure using PPC are −243.34, −40.30, and 230.17 kcal/mol, respectively, as compared to −150.14, −37.38, and 133.44 kcal/mol for the rank one structure (see Table S4 of the Supporting Information). By including bridging water molecules, the three corresponding energy terms for the native structure are −251.69, −43.69, and 226.47 kcal/mol, as compared to −173.60, −40.45, and 166.50 kcal/mol for the rank one

structure. MM/PBSA successfully recognizes the correct binding pose in the presence of structural water molecules with the binding free energy of −75.76 kcal/mol compared with −54.23 kcal/mol for the rank one structure. On the contrary, MM/PBSA based on the ensemble averaging without considering bridging-water molecules fails to predict the correct binding pose of 1FJS with the PPC model. It is much the same for 3CLA and 4CLA. After explicitly including bridging waters, MM/PBSA with PPC achieves success for all the test systems. Therefore, the protein−ligand binding poses are better determined by explicitly treating bridging water molecules. It is of great importance to include the effects of both bridging water molecules and electronic polarization in MM/PBSA calculations.

E. Compare Residue-Based Binding Free Energies between the Amber ff99SB and PPC Charge Models. For 1FJS, after explicitly treating bridging water molecules in MM/PBSA calculation, the PPC model correctly identifies the binding pose, whereas the Amber ff99SB charge model fails (compare Figure 1i and 1j). We further decompose the total binding free energy of the protein−ligand complex into contributions from each residue (the bridging water molecule is taken as a residue of protein). The residue-based free-energy decomposition has been rigorously established in the free energy perturbation formalism and represents the foundation of any quantitative structure−activity relationship.[64,65] The primary residues which make contributions to the binding free energy larger than 1.0 kcal/mol are shown in Figure 4. For

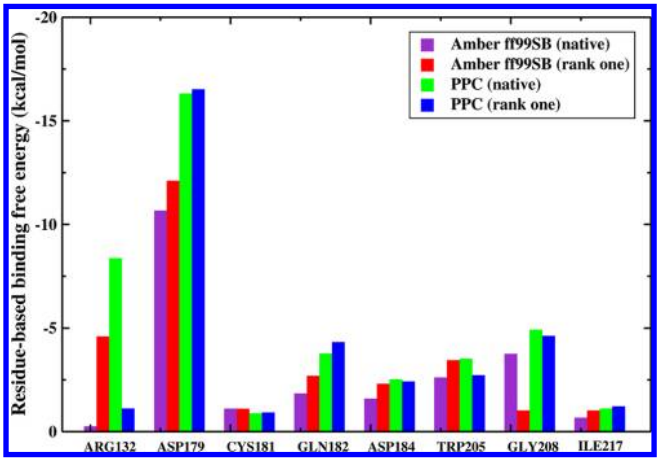

Figure 4. Decomposed residue-based binding free energies (in kcal/mol) between the ligand and key residues for the structure of 1FJS.

the Amber ff99SB charge model, except CYS181 and GLY208, the calculated binding free energies for all other 6 residues in the rank one structure are more favorable than those in the native structure, which accounts for the failure of predicting the correct binding pose based on the Amber ff99SB force field.

On the contrary, the calculated residue-based free energies in the native structure using PPC are more attractive than those in the rank one structure for four residues (ARG132, ASP184, TRP205, and GLY208). For ARG132, the calculated free energies with the Amber ff99SB charges for the native and rank one conformations are −0.23 and −4.57 kcal/mol, respectively, as compared to the PPC results of −8.35 and −1.03 kcal/mol. As for the other three primary residues (ASP179, GLN182, and ILE217), although the calculated free energies in the rank one structure are more favorable than the native structure for both the Amber ff99SB and PPC charge models, PPC consistently shrinks the margins of residue-based binding free energies between the native and rank one structures. For instance, the calculated free energies of ASP179 are −10.65 and −12.08 kcal/mol for the native and rank one binding poses, respectively, using Amber ff99SB charges. The gap of 1.43 kcal/mol is considerably larger than 0.23 kcal/mol using PPC (the corresponding binding free energies are −16.27 and −16.50 kcal/mol, respectively). The results show that using PPC in MM/PBSA calculations can better differentiate the native structure from the decoy structures. The electronic polarization effect not only impacts the tightness between residues and ligand during MD simulation, but also provides more accurate evaluation of binding free energies for the protein−ligand complexes.

4. CONCLUSIONS

In this work, we employed a systematic study of eight protein−ligand complexes, for which Autodock could not predict their binding poses correctly. We incorporate the PPC charge model into the MM/PBSA method to rescore the top-rank binding poses of those systems, and compare with the value obtained from the native binding structure. Different sampling techniques including single minimized conformation and multiple MD snapshots are used to test the performance of MM/PBSA combined with the PPC model. By explicitly including bridging water molecules in MM/PBSA calculations using PPC charges, the ensemble-averaged free energy correctly ranks the binding poses for these eight systems. In contrast, MM/PBSA calculations with the nonpolarizable Amber ff99SB charges failed in four systems. Our study underscores that the effects of bridging water molecules and the electronic polarization are both crucial to accurately predict the protein−ligand binding affinity. Furthermore, the free energy averaging over multiple MD snapshots is a more accurate approach than that calculated on a single minimized protein−ligand complex, although much more computational cost is needed.

The next study will focus on developing a reliable method to locate the possible position of the bridging water molecules, and an efficient way to incorporate the electronic polarization effect in empirical scoring functions. Research along these lines is currently underway at our laboratory.

■ ASSOCIATED CONTENT

Supporting Information

Partial atomic charges of all eight inhibitors, number of TIP3P waters added, along with the number and type of counterions added to each complex, and decomposition of the calculated MM/PBSA free energies based on the single minimized structure and 50 snapshots selected from MD simulation. This information is available free of charge via the Internet at http://pubs.acs.org

■ AUTHOR INFORMATION

Corresponding Author

*E-mail: xiaohe@phy.ecnu.edu.cn (X.H.); john.zhang@nyu.edu (J.Z.H.Z.).

Notes

The authors declare no competing financial interest.

■ ACKNOWLEDGMENTS

This work was supported by the National Natural Science Foundation of China (Grants No. 10974054 and 20933002) and Shanghai PuJiang program (09PJ1404000). We also thank the Computational Center of ECNU for providing us computational time.

■ REFERENCES

(1) Friesner, R. A.; Banks, J. L.; Murphy, R. B.; Halgren, T. A.; Klicic, J. J.; Mainz, D. T.; Repasky, M. P.; Knoll, E. H.; Shelley, M.; Perry, J. K.; Shaw, D. E.; Francis, P.; Shenkin, P. S. Glide: A new approach for rapid, accurate docking and scoring. 1. Method and assessment of docking accuracy. *J. Med. Chem.* **2004**, *47*, 1739−1749.

(2) Morris, G. M.; Goodsell, D. S.; Halliday, R. S.; Huey, R.; Hart, W. E.; Belew, R. K.; Olson, A. J. Automated docking using a Lamarckian genetic algorithm and an empirical binding free energy function. *J. Comput. Chem.* **1998**, *19*, 1639−1662.

(3) Rarey, M.; Kramer, B.; Lengauer, T.; Klebe, G. A fast flexible docking method using an incremental construction algorithm. *J. Mol. Biol.* **1996**, *261*, 470−489.

(4) Jones, G.; Willett, P.; Glen, R. C.; Leach, A. R.; Taylor, R. Development and validation of a genetic algorithm for flexible docking. *J. Mol. Biol.* **1997**, *267*, 727−748.

(5) Wang, R. X.; Lu, Y. P.; Wang, S. M. Comparative evaluation of 11 scoring functions for molecular docking. *J. Med. Chem.* **2003**, *46*, 2287−2303.

(6) Cummings, M. D.; DesJarlais, R. L.; Gibbs, A. C.; Mohan, V.; Jaeger, E. P. Comparison of automated docking programs as virtual screening tools. *J. Med. Chem.* **2005**, *48*, 962−976.

(7) Kontoyianni, M.; McClellan, L. M.; Sokol, G. S. Evaluation of docking performance: comparative data on docking algorithms. *J. Med. Chem.* **2004**, *47*, 558−565.

(8) Kontoyianni, M.; Sokol, G. S.; McClellan, L. M. Evaluation of library ranking efficacy in virtual screening. *J. Comput. Chem.* **2005**, *26*, 11−22.

(9) Perola, E.; Walters, W. P.; Charifson, P. S. A detailed comparison of current docking and scoring methods on systems of pharmaceutical relevance. *Proteins* **2004**, *56*, 235−249.

(10) Wang, R. X.; Lu, Y. P.; Fang, X. L.; Wang, S. M. An extensive test of 14 scoring functions using the PDBbind refined set of 800 protein-ligand complexes. *J. Chem. Inf. Comput. Sci.* **2004**, *44*, 2114−2125.

(11) Bissantz, C.; Folkers, G.; Rognan, D. Protein-based virtual screening of chemical databases. 1. Evaluation of different docking/scoring combinations. *J. Med. Chem.* **2000**, *43*, 4759−4767.

(12) Paul, N.; Rognan, D. ConsDock, A new program for the consensus analysis of protein-ligand interactions. *Proteins* **2002**, *47*, 521−533.

(13) Weis, A.; Katebzadeh, K.; Soderhjelm, P.; Nilsson, I.; Ryde, U. Ligand affinities predicted with the MM/PBSA Method: Dependence on the Simulation Method and the Force Field. *J. Med. Chem.* **2006**, *49*, 6596−6606.

(14) Wang, J. M.; Hou, T. J.; Xu, X. J. Recent advances in free energy calculations with a combination of molecular mechanics and continuum models. *Curr. Comput.-Aided Drug Des.* **2006**, *2*, 287−306.

(15) Wang, W.; Donini, O.; Reyes, C. M.; Kollman, P. A. Biomolecular simulations: Recent developments in force fields, simulations of enzyme catalysis, protein−ligand, protein−protein, and protein−nucleic acid noncovalent interactions. *Annu. Rev. Biophys. Biomol. Struct.* **2001**, *30*, 211−243.

(16) Kollman, P. A.; Massova, I.; Reyes, C.; Kuhn, B.; Huo, S. H.; Chong, L.; Lee, M.; Lee, T.; Duan, Y.; Wang, W.; Donini, O.; Cieplak, P.; Srinivasan, J.; Case, D. A.; Cheatham, T. E. Calculating structures and free energies of complex molecules: Combining molecular mechanics and continuum models. *Acc. Chem. Res.* **2000**, *33*, 889−897.

(17) Muegge, I. Effect of ligand volume correction on PMF scoring. *J. Comput. Chem.* **2001**, *22*, 418−425.

(18) Muegge, I.; Martin, Y. C. A general and fast scoring function for protein-ligand interactions: A simplified potential approach. *J. Med. Chem.* **1999**, *42*, 791−804.

(19) Gohlke, H.; Hendlich, M.; Klebe, G. Knowledge-based scoring function to predict protein−ligand interactions. *J. Mol. Biol.* **2000**, *295*, 337−356.

(20) Lyne, P. D.; Lamb, M. L.; Saeh, J. C. Accurate prediction of the relative potencies of members of a series of kinase inhibitors using molecular docking and MM-GBSA scoring. *J. Med. Chem.* **2006**, *49*, 4805−4808.

(21) Guimaraes, C. R. W.; Cardozo, M. MM-GB/SA rescoring of docking poses in structure-based lead optimization. *J. Chem. Inf. Model.* **2008**, *48*, 958−970.

(22) Kuhn, B.; Gerber, P.; Schultz-Gasch, T.; Stahl, M. Validation and use of the MM-PBSA approach for drug discovery. *J. Med. Chem.* **2005**, *48*, 4040−4048.

(23) Hou, T. J.; Wang, J. M.; Li, Y. Y.; Wang, W. Assessing the performance of the MM/PBSA and MM/GBSA methods. 1.The accuracy of binding free energy calculations based on molecular dynamics simulations. *J. Chem. Inf. Model.* **2011**, *51*, 69−82.

(24) Hou, T. J.; Wang, J. M.; Li, Y. Y.; Wang, W. Assessing the performance of the molecular mechanics Poisson Boltzmann surface area and molecular mechanics generalized Born surface area methods. II. The accuracy of ranking poses generated from docking. *J. Comput. Chem.* **2011**, *32*, 866−877.

(25) Zhang, D. W.; Zhang, J. Z. H. Molecular fractionation with conjugate caps for full quantum mechanical calculation of protein−molecule interaction energy. *J. Chem. Phys.* **2003**, *119*, 3599−3606.

(26) Gao, A. M.; Zhang, D. W.; Zhang, J. Z. H.; Zhang, Y. K. An efficient linear scaling method for ab initio calculation of electron density of proteins. *Chem. Phys. Lett.* **2004**, *394*, 293−297.

(27) Mei, Y.; Ji, C. G.; Zhang, J. Z. H. A new quantum method for electrostatic solvation energy of protein. *J. Chem. Phys.* **2006**, *125*, No. 094906.

(28) Ji, C. G.; Mei, Y.; Zhang, J. Z. H. Developing polarized protein-specific charges for protein dynamics: MD free energy calculation of pK_a shifts for Asp26/Asp20 in thioredoxin. *Biophys. J.* **2008**, *95*, 1080−1088.

(29) Tong, Y.; Mei, Y.; Zhang, J. Z. H.; Duan, L. L.; Zhang, Q. G. Quantum calculation of protein solvation and protein-ligand binding free energy for HIV-1 protease/water complex. *J. Theor. Comput. Chem.* **2009**, *8*, 1265−1279.

(30) Tong, Y.; Mei, Y.; Li, Y. L.; Ji, C. G.; Zhang, J. Z. H. Electrostatics polarization makes a substantial contribution to the free energy of avidin−biotin binding. *J. Am. Chem. Soc.* **2010**, *132*, 5137−5142.

(31) McConkey, B. J.; Sobolev, V.; Edelman, M. The performance of current methods in ligand-protein docking. *Curr. Sci.* **2002**, *83*, 845−856.

(32) de Graaf, C.; Pospisil, P.; Pos, W.; Folkers, G.; Vermeulen, N. P. E. Binding mode prediction of cytochrome P450 and thymidine kinase protein-ligand complexes by consideration of water and rescoring in automated docking. *J. Med. Chem.* **2005**, *48*, 2308−2318.

(33) Poornima, C. S.; Dean, P. M. Hydration in drug design. 1. Multiple hydrogen-bonding features of water molecules in mediating protein-ligand interactions. *J. Comput.-Aided Mol. Des.* **1995**, *9*, 500−512.

(34) Poornima, C. S.; Dean, P. M. Hydration in drug design. 2. Influence of local site surface shape on water binding. *J. Comput.-Aided Mol.Des.* **1995**, *9*, 513−520.

(35) Poornima, C. S.; Dean, P. M. Hydration in drug design. 3. Conserved water molecules at the ligand-binding sites of homologous proteins. *J. Comput.-Aided Mol. Des.* **1995**, *9*, 521−531.

(36) Friesner, R. A.; Murphy, R. B.; Repasky, M. P.; Frye, L. L.; Greenwood, J. R.; Halgren, T. A.; Sanschagrin, P. C.; Mainz, D. T. Extra precision Glide: Docking and scoring incorporating a model of hydrophobic enclosure for protein−ligand complexes. *J. Med. Chem.* **2006**, *49*, 6177−6196.

(37) Young, T.; Abel, R.; Kim, B.; Berne, B. J.; Friesner, R. A. Motifs for molecular recognition exploiting hydrophobic enclosure in protein−ligand binding. *Proc. Natl. Acad. Sci. U.S.A.* **2007**, *104*, 808−813.
(38) Abel, R.; Young, T.; Farid, R.; Berne, B. J.; Friesner, R. A. Role of the active-site solvent in the thermodynamics of factor Xa ligand binding. *J. Am. Chem. Soc.* **2008**, *130*, 2817−2831.
(39) Rarey, M.; Kramer, B.; Lengauer, T.; Klebe, G. The particle concept: placing discrete water molecules during protein-ligand docking predictions. *Proteins* **1999**, *34*, 17−28.
(40) Schnecke, V.; Kuhn, L. A. Virtual screening with solvation and ligand-induced complementarity. *Perspect. Drug Discovery Des.* **2000**, *20*, 171−190.
(41) Osterberg, F.; Morris, G. M.; Sanner, M. F.; Olson, A. J.; Goodsell, D. S. Automated docking to multiple target structures: incorporation of protein mobility and structural water heterogeneity in AutoDock. *Proteins* **2002**, *46*, 34−40.
(42) Verdonk, M. L.; Chessari, G.; Cole, J. C.; Hartshorn, M. J.; Murray, C. W. Modeling water molecules in protein-ligand docking using GOLD. *J. Med. Chem.* **2005**, *48*, 6504−6515.
(43) Case, D. A.; Cheatham, T. E.; Darden, T.; Gohlke, H.; Luo, R.; Merz, K. M.; Onufriev, A.; Simmerling, C.; Wang, B.; Woods, R. J. The Amber biomolecular simulation programs. *J. Comput. Chem.* **2005**, *26*, 1668−1688.
(44) Hornak, V.; Abel, R.; Okur, A.; Strockbine, B.; Roitberg, A.; Simmerling, C. Comparison of multiple Amber force fields and development of improved protein backbone parameters. *Proteins: Struct., Funct., Bioinf.* **2006**, *65*, 712−725.
(45) Wang, J. M.; Wang, W.; Kollman, P. A.; Case, D. A. Automatic atom type and bond type perception in molecular mechanical calculations. *J. Mol. Graphics Modell.* **2006**, *25*, 247−260.
(46) Wang, J. M.; Wolf, R. M.; Caldwell, J. W.; Kollman, P. A.; Case, D. A. Development and testing of a general Amber force field. *J. Comput. Chem.* **2004**, *25*, 1157−1174.
(47) Bren, U.; Hodoscek, M.; Koller, J. Development and validation of empirical force field parameters for netropsin. *J. Chem. Inf. Model.* **2005**, *45*, 1546−1552.
(48) Udommaneethanakit, T.; Rungrotmongkol, T.; Bren, U.; Frecer, V.; Stanislav, M. Dynamic behavior of avian influenza A virus neuraminidase subtype H5N1 in complex with oseltamivir, zanamivir, peramivir, and their phosphonate analogues. *J. Chem. Inf. Model.* **2009**, *49*, 2323−2332.
(49) Frisch, M. J.; Trucks, G. W.; Schlegel, H. B.; Scuseria, G. E.; Robb, M. A.; Cheeseman, J. R.; Scalmani, G.; Barone, V.; Mennucci, B.; Petersson, G. A.; Nakatsuji, H.; Caricato, M.; Li, X.; Hratchian, H. P.; Izmaylov, A. F.; Bloino, J.; Zheng, G.; Sonnenberg, J. L.; Hada, M.; Ehara, M.; Toyota, K.; Fukuda, R.; Hasegawa, J.; Ishida, M.; Nakajima, T.; Honda, Y.; Kitao, O.; Nakai, H.; Vreven, T.; Montgomery, J. A., Jr.; Peralta, J. E.; Ogliaro, F.; Bearpark, M.; Heyd, J. J.; Brothers, E.; Kudin, K. N.; Staroverov, V. N.; Keith, T.; Kobayashi, R.; Normand, J.; Raghavachari, K.; Rendell, A.; Burant, J. C.; Iyengar, S. S.; Tomasi, J.; Cossi, M.; Rega, N.; Millam, J. M.; Klene, M.; Knox, J. E.; Cross, J. B.; Bakken, V.; Adamo, C.; Jaramillo, J.; Gomperts, R.; Stratmann, R. E.; Yazyev, O.; Austin, A. J.; Cammi, R.; Pomelli, C.; Ochterski, J. W.; Martin, R. L.; Morokuma, K.; Zakrzewski, V. G.; Voth, G. A.; Salvador, P.; Dannenberg, J. J.; Dapprich, S.; Daniels, A. D.; Farkas, O.; Foresman, J. B.; Ortiz, J. V.; Cioslowski, J.; Fox, D. J. *Gaussian 09*, revision B.01; Gaussian, Inc.: Wallingford, CT, 2010.
(50) Rocchia, W.; Sridharan, S.; Nicholls, A.; Alexov, E.; Chiabrera, A.; Honig, B. Rapid grid-based construction of the molecular surface and the use of induced surface charge to calculate reaction field energies: Applications to the molecular systems and geometric objects. *J. Comput. Chem.* **2002**, *23*, 128−137.
(51) Cornell, W. D.; Cieplak, P.; Bayly, C. I.; Gould, I. R.; Merz, K. M.; Ferguson, D. M.; Spellmeyer, D. C.; Fox, T.; Caldwell, J. W.; Kollman, P. A. A second generation force field for the simulation of proteins, nucleic acids, and organic molecules. *J. Am. Chem. Soc.* **1995**, *117*, 5179−5197.
(52) Bayly, C. I.; Cieplak, P.; Cornell, W.; Kollman, P. A. A well-behaved electrostatic potential based method using charge restraints for deriving atomic charges: The RESP model. *J. Phys. Chem.* **1993**, *97*, 10269−10280.
(53) Cornell, W. D.; Cieplak, P.; Bayly, C. I.; Kollmann, P. A. Application of RESP charges to calculate conformational energies, hydrogen bond energies, and free energies of solvation. *J. Am. Chem. Soc.* **1993**, *115*, 9620−9631.
(54) Darden, T.; York, D.; Pedersen, L. Particle mesh Ewald: An *N*−log(*N*) method for Ewald sums in large systems. *J. Chem. Phys.* **1993**, *98*, 10089−10093.
(55) Ryckaert, J. P.; Ciccotti, G.; Berendsen, H. J. C. Numerical-integration of Cartesian equations of motion of a system with constraints molecular-dynamics of *N*-alkanes. *J. Comput. Phys.* **1977**, *23*, 327−341.
(56) Pastor, R. W.; Brooks, B. R.; Szabo, A. An analysis of the accuracy of Langevin and molecular-dynamics algorithms. *Mol. Phys.* **1988**, *65*, 1409−1419.
(57) Gohlke, H.; Case, D. A. Converging free energy estimates: MM-PB(GB)SA studies on the protein−protein complex Ras−Raf. *J. Comput. Chem.* **2004**, *25*, 238−250.
(58) Weiser, J.; Shenkin, P. S.; Still, W. C. Approximate atomic surfaces from linear combinations of pairwise overlaps (LCPO). *J. Comput. Chem.* **1999**, *20*, 217−230.
(59) Li, Y.; Ji, C. G.; Xu, W. X.; Zhang, J. Z. H. Dynamical stability and assembly cooperativity of beta-sheet amyloid oligomers—Effect of polarization. *J. Phys. Chem. B.* **2012**, *116*, 13368−13373.
(60) Åqvist, J.; Medina, C.; Samuelsson, J. E. A new method for predicting binding affinity in computer-aided drug design. *Protein Eng.* **1994**, *7*, 385−391.
(61) Bren, U.; Janezic, D. Individual degrees of freedom and the solvation properties of water. *J. Chem. Phys.* **2012**, *137*, 024108.
(62) Lee, F. S.; Chu, Z. T.; Bolger, M. B.; Warshel, A. Calculations of antibody−antigen interactions: Microscopic and semi-microscopic evaluation of the free energies of binding of phosphorylcholine analogs to McPC603. *Protein Eng.* **1992**, *5*, 215−228.
(63) Bren, U.; Oostenbrink, C. Cytochrome P450 3A4 inhibition by ketoconazole: Tackling the problem of ligand cooperativity using molecular dynamics simulations and free-energy calculations. *J. Chem. Inf. Model* **2012**, *52*, 1573−1582.
(64) Bren, U.; Martinek, V.; Florian, J. Decomposition of the solvation free energies of deoxyribonucleoside triphosphates using the free energy perturbation method. *J. Phys. Chem. B.* **2006**, *110*, 12782−12788.
(65) Bren, M.; Florian, J.; Mavri, J.; Bren, U. Do all pieces make a whole? Thiele cumulants and the free energy decomposition. *Theor. Chem. Acc.* **2007**, *117*, 535−540.